Appl. Phys. B 40, 1–7 (1986)

Applied Physics B Photophysics and Laser Chemistry



# Multiplex Rotational CARS of $N_2$, $O_2$, and CO with Excimer Pumped Dye Lasers: Species Identification and Thermometry in the Intermediate Temperature Range with High Temporal and Spatial Resolution

B. Dick and A. Gierulski

Max-Planck-Institut für Biophysikalische Chemie, Abteilung Laserphysik, Am Fassberg, D-3400 Göttingen, Fed. Rep. Germany

Received 9 December 1985/Accepted 21 February 1981

**Abstract.** Pure rotational CARS spectra of $N_2$, $O_2$, air, and CO have been obtained using excimer laser pumped dye-lasers. The combination of the folded BOXCARS phase matching geometry with the broad-band laser multiplex method allowed high spatial and temporal resolution. Species and concentration analysis as well as thermometry up to 700 K is demonstrated, and possible applications are discussed.

**PACS:** 42.65

Diagnostic tools based on nonlinear optical processes have found increasing application for the study of reactive media, particularly in combustion processes [1]. Especially coherent anti-Stokes Raman scattering (CARS) is now a well established method [2–5]. Its main application in combustion studies today is thermometry in flames employing the vibrational Raman resonance of molecular nitrogen. The CARS spectrum of this resonance shows the $Q$-branches ($\Delta J=0$) of the transitions $v=0 \rightarrow v=1$ and $v=1 \rightarrow v=2$. For each transition in a CARS spectrum the intensity depends on the population difference between the corresponding levels and is consequently temperature dependent. The great number of closely spaced rotational lines of these $Q$-branches can be resolved when the CARS spectrum is scanned with narrow-band lasers [6, 7]. However, many applications require a multiplex method which yields complete CARS spectra with a single laser shot. This method has a typical resolution of 1 $cm^{-1}$ determined by the monochromator and diode array combination. Therefore, individual rotational lines within the $Q$-branch are usually not resolved, and only the envelope can be obtained. Comparison of these spectra with computer-generated band shapes yield temperatures in good agreement with thermocouple measurements [7–10]. For temperatures below 1000 K, however, the population in the $v=1$ level is so small that the "hot band" $v=1 \rightarrow v=2$ vanishes in the wing of the "cold band" $v=0 \rightarrow v=1$. The shape of this cold band is not very sensitive to temperature changes below 1000 K. Thus it appears that vibrational CARS is not very useful in this lower temperature range.

One alternative is rotational CARS. For this process the selection rules are the same as for rotational Raman scattering, namely $\Delta v=0$ and $\Delta J=2$. Consequently, the CARS spectrum of a rotator without centrifugal distortion consists of equidistant lines with spacing $4B$, where $B$ is the rotational constant. In molecular nitrogen this line spacing is about 8 $cm^{-1}$. Therefore it should be easy to resolve individual lines even in the multiplex mode. Temperature fits are normally based on the assumption of a Boltzmann distribution within the level manifold of interest. In this case the population of a rotational level with quantum number $J$ is

$$N(J)=\frac{1}{Q} g_J(2J+1)\exp[-E(J)/kT]. \quad (1)$$

In this expression, $g_J$ is the nuclear spin degeneracy factor, $E(J)$ is the energy of the rotational level with

quantum number $J$

$$E(J)=BJ(J+1)+DJ^2(J+1)^2 \tag{2}$$

and $Q$ is the rotational partition function. In molecular nitrogen at a temperature of 300 K the level with the largest population is $J=6$, whereas for $T=1000$ K it is $J=12$. The strongest CARS lines are calculated to be $J=8 \rightarrow J=10$ at 300 K and $J=18 \rightarrow J=20$ at 1000 K. Thus a considerable shift of spectral intensities is expected in this temperature range, promising good sensitivity for thermometry.

Despite these interesting features only very few studies of rotational CARS have been performed to date. One great obstacle is the fact that except for hydrogen [11, 12] the Stokes shift for pure rotational Raman transitions is very small, namely from 10 $cm^{-1}$ to about 250 $cm^{-1}$. This makes it very difficult to separate the CARS signal from the strong laser beams. Nevertheless, rotational CARS spectra of air in scanned mode were obtained with colinear beams [13, 14]. To reject the strong laser light a narrow spectral window for the signal had to be scanned synchronously with the laser. Goss et al. [15] used a non-phasematched configuration with two laser beams crossing under a small angle. A phase-matched configuration with complete spatial separation of the signal from the lasers, called folded BOXCARS, was developed by Shirley et al. [16]. This configuration enabled the application of the multiplex technique to rotational CARS: Alden et al. [17] and Zheng et al. [18] showed rotational CARS and CSRS (coherent Stokes Raman scattering) spectra of air. Both CARS and CSRS spectra yield the same information in accordance with theory. Snow et al. [19] studied the spatial resolution in a large angle BOXCARS configuration. We know of only two temperature dependent studies using rotational CARS: Murphy and Chang [20] investigated nitrogen below room temperature, and Zheng et al. [21] discussed rotational CARS in flames in comparison to vibrational CARS.

All these multiplex rotational CARS studies use an apparatus based on a Nd:YAG laser. Its second harmonic serves as the first input beam for the CARS process, whereas the second beam is a broad-band dye laser pumped by the third harmonic of the Nd:YAG laser. Our apparatus employs an alternative concept in which both lasers interacting in the CARS process are dye lasers simultaneously pumped by a strong excimer laser.

## 1. Theory

The intensity distribution in the CARS spectrum obtained in multiplex mode is given by [22]

$$I_{\mathrm{CARS}}(2\omega_L-\omega_S)=KI_LI_L'I_S(\omega_S)\cdot|\chi|^2. \tag{3}$$

$I_L$ and $I_L'$ are the intensities of the two narrowband pumplaser beams, $I_S(\omega_S)$ is the spectrum of the broadband dye laser, $K$ is a constant containing phasematching factors, and $\chi$ is the nonlinear susceptibility of the sample. The latter is the sum of resonant terms for all allowed transitions $J\rightarrow J'$ and a nonresonant background term

$$\chi=\sum_{JJ'}\frac{A_{JJ'}}{\omega_{JJ'}-\omega_L+\omega_S+\mathrm{i}\Gamma_{JJ'}}+\chi^{NR}. \tag{4}$$

The resonant terms are written as complex Lorentzians with center frequencies $\omega_{JJ'}=(E_J-E_{J'})/\hbar$, line widths $\Gamma_{JJ'}$, and amplitudes $A_{JJ'}$. This line shape must be convoluted with the Doppler distribution and the finite linewidth of the pump-laser beams. However, for the following discussion only the amplitudes $A_{JJ'}$ are relevant. When the resonance frequencies are well separated from each others (several linewidths $\Gamma_{JJ'}$), and when the nonresonant susceptibility $\chi^{NR}$ is small, no interference will occur and each resonance will appear in the spectrum as a peak with a height determined by $|A_{JJ'}|^2$. The amplitude factor $A_{JJ'}$ contains matrix elements of the Raman transition operator for the two Raman processes involved in the CARS process, multiplied by the population difference of the two levels coupled by the Raman resonance, and summed over all degenerate sublevels

$$A_{JJ'}=\sum_{MM'}(N_{JM}-N_{J'M'})\times\langle JM|\hat{e}_L\underline{R}\hat{e}_S|J'M'\rangle\langle J'M'|\hat{e}_{L'}\underline{R}\hat{e}_A|JM\rangle. \tag{6}$$

$\underline{R}$ is the Raman transition tensor, i.e. the polarizability tensor of the molecule in its electronic ground state, expressed in laboratory coordinates. The unit polarization vectors $\hat{e}_L$, $\hat{e}_S$, $\hat{e}_{L'}$, and $\hat{e}_A$ correspond to the four photons of first pump, Stokes, second pump, and generated anti-Stokes frequency that take part in the CARS process in this time ordering.

One way to calculate the matrix element is to express the tensor product in the spherical tensor notation

$$\hat{e}_1\underline{R}\cdot\hat{e}_2=\sum_{j=0}^{2}\sum_{m=-j}^{j}(-1)^mR_m^j(\hat{e}_1\otimes\hat{e}_2)^j_{-m}. \tag{7}$$

The tensor components $R_m^j$ in the laboratory frame are related to those in the molecular frame, $r_k^j$, through Wigner rotation matrices

$$R_m^j=\sum_k D_{mk}^j(\Omega)r_k^j. \tag{8}$$

Linear molecules have only the two non-zero tensor components

$$r_0^0=-(r_{\|}+2r_{\perp})/\sqrt{3};\quad r_0^2=\sqrt{2/3}(r_{\|}-r_{\perp}). \tag{9}$$

Here $r_{\|}$ and $r_{\perp}$ denote the component parallel and perpendicular to the molecular axis. The tensor $r_0^0$

contributes only to transitions with $\Delta J=0$, e.g. the $Q$-branch of vibrational CARS transitions. In pure rotational CARS a transition with $\Delta J=0$ corresponds to the Rayleigh line. The tensor $r_0^2$ yields contributions to $\Delta J=0$ and $\Delta J=2$ transitions. For the latter the final result of (6) is

$$A_{J,J+2}=\left(\frac{N(J)}{2J+1}-\frac{N(J+2)}{2J+5}\right)\times\frac{1}{5}\cdot(r_0^2)^2\frac{(J+1)(J+2)}{2J+3}\cdot F,$$
$$F=\tfrac{1}{2}(\hat{e}_L\cdot\hat{e}_{L'})(\hat{e}_S\cdot\hat{e}_A)+\tfrac{1}{12}(\hat{e}_L\cdot\hat{e}_S)(\hat{e}'_L\cdot\hat{e}_A)+\tfrac{1}{12}(\hat{e}_L\cdot\hat{e}_A)(\hat{e}'_L\cdot\hat{e}_S). \quad (10)$$

It is interesting to note that all polarization information reduces to a single factor which affects all amplitudes in the same way. The relative line intensities in rotational CARS are, therefore, not influenced by the polarization of the lasers. [The polarization expression describing the general result for a CARS experiment involving the time ordering $\omega_L-\omega_S+\omega'_L=\omega_A$ with four distinguishable photons is

$$F=\tfrac{1}{2}(\hat{e}_L\cdot\hat{e}'_L)(\hat{e}_S\cdot\hat{e}_A)+\tfrac{1}{2}(\hat{e}_L\cdot\hat{e}_A)(\hat{e}'_L\cdot\hat{e}_S)-\tfrac{1}{3}(\hat{e}_L\cdot\hat{e}_S)(\hat{e}'_L\cdot\hat{e}_A). \quad (11)$$

In our experiment this time ordering cannot be distinguished from the time ordering with the photons of energy $\omega_L$ from the two pump beams interchanged. Therefore, the polarization factors for both processes were averaged in (10).]

When the level populations obey a Boltzmann distribution the amplitude factor takes the form

$$A_{J,J+2}=N(J)\cdot[1-\exp(-\hbar\omega_{J,J+2}/kT)]\times\frac{(J+1)(J+2)}{(2J+1)(2J+3)}(r_0^2)^2\cdot F/5. \quad (12)$$

This equation was used in all calculations of relative line intensities for spectrum simulations and temperature fits. For spectrum simulations the narrow Lorentzian spectrum was convoluted with a Gaussian spectrometer function with 1.0 $cm^{-1}$ width, corresponding to the resolution of our apparatus.

## 2. Experimental

The schematic of our CARS apparatus is shown in Fig. 1. In contrast to the majority of the systems capable of multiplex CARS measurements it did not use a Nd:YAG laser as the pumping source. Instead, both the CARS pump beam and the broad-band Stokes beam were produced from dye lasers simultaneously pumped by a XeCl excimer level (Lambda Physik EMG 201MSC) with 400 mJ pulse energy. Typical pulses from the narrow-band dye laser/amplifier combination (Lambda Physik FL2002) had 20 mJ energy in a 0.1 $cm^{-1}$ bandwidth at 534 nm with coumarine 307 dye. The broad-band dye laser was a prototype by Lambda Physik (model FL1002C) with tunable bandwidth and center frequency. Typical pulses of the broad-band system in this work were

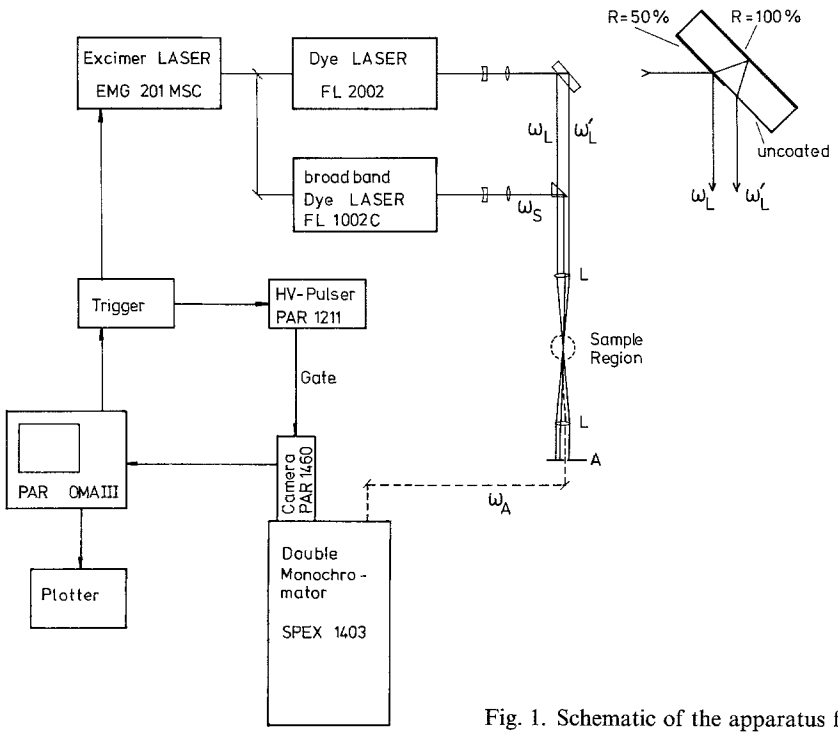


Fig. 1. Schematic of the apparatus for multiplex rotational CARS measurements

250 $cm^{-1}$ wide at 540 nm and 15 mJ energy using the dye coumarine 153.

The folded BOXCARS configuration [16, 23] was used to spatially separate the signal from the intense dye laser beams. A plane parallel plate with special dielectric coatings split the narrow-band laser beam into two exactly parallel propagating beams (Fig. 1). This ensured that both beams were optimally focused to a common spot into the sample region by the lens $L_1$ ($f=300$ mm). This considerably simplified the adjustment of the third beam from the broad-band laser. The telescopes in both dye laser beams enlarged the beam cross sections by a factor of 3 to protect the coatings and allowed to correct for the different divergence in the dye laser beams.

Behind the sample region the beams were recollimated and the CARS signal beam selected with an aperture. The spectrum of the CARS signal was dispersed by a 3/4 m double monochromator (Spex model 1403) and observed with an optical multichannel analyser camera with image intensifier (PAR model 1460). Due to crosstalk between adjacent diodes the resolution of the complete setup was limited to ca. 4 channels of the camera, corresponding to ca. 1 $cm^{-1}$. The image from the camera was processed by a microcomputer system (OMA III, PAR), stored on diskette, and plotted. This microcomputer also generated the trigger pulses for the excimer laser and the high voltage pulser (PAR 1211) which gated the image intensifier. For adjustment and normal operation the system was run at a repetition rate of 3–5 Hz. Maximum repetition rate of the laser system was 80 Hz. The OMA system can be synchronized to this speed when only the 700 channels covered by the image intensifier are processed.

## 3. Results and Discussion

Figure 2 shows the spectra of $N_2$ (2 atm), $O_2$ (1 atm), and CO (600 Torr) obtained at room temperature with gas cells placed into the sample region. For $N_2$ the ratio of the nuclear spin degeneracy factors [24] $g$(even) : $g$(odd) is 2 : 1 leading to an intensity alteration of approximately 4 : 1 for even and odd lines. In $O_2$ this ratio is 0 : 1 and the even lines are missing altogether. Finally, in CO the nuclear spin wavefunction has no symmetry and all transitions have equal weight. Below each experimental spectrum the corresponding theoretical spectrum is shown.

The applicability of rotational CARS to species and concentration analysis is demonstrated in Fig. 3 show-

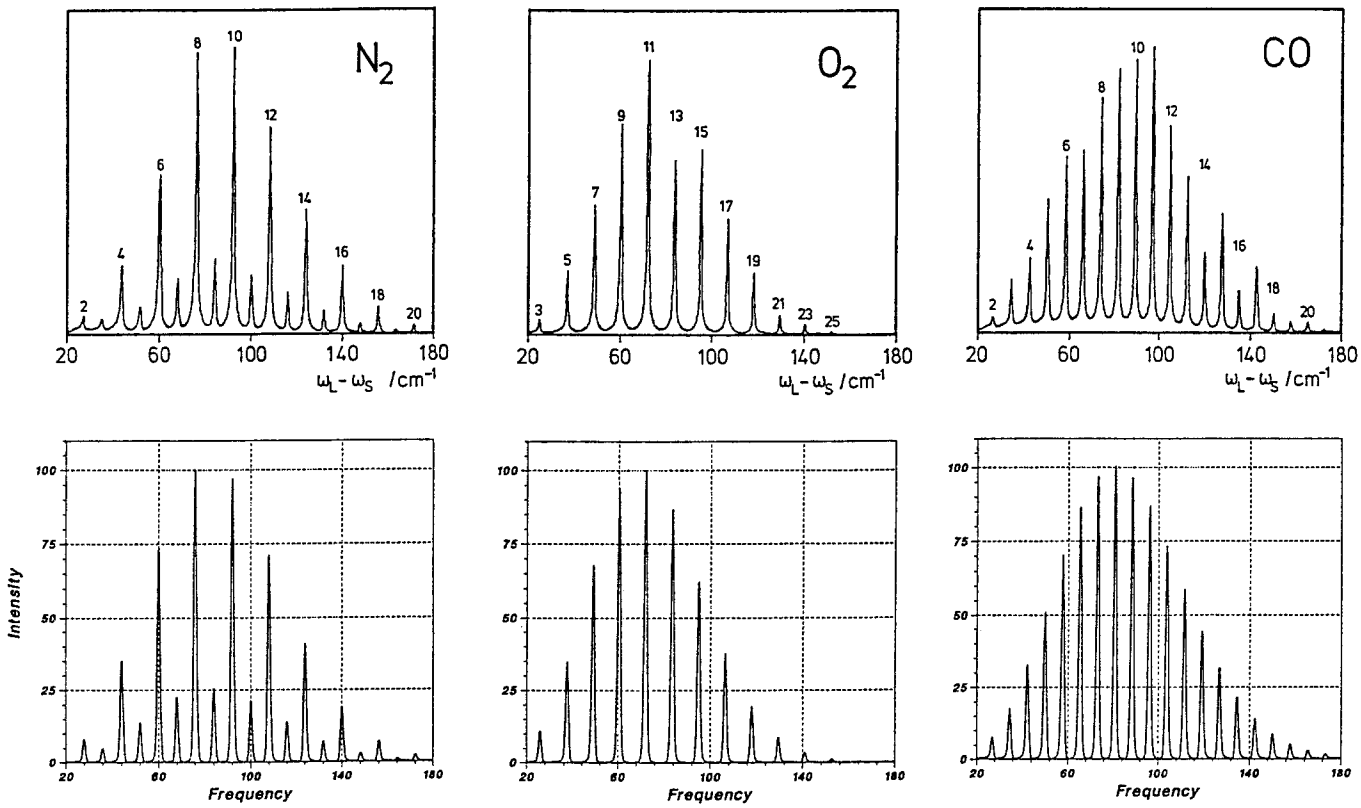


Fig. 2. Upper part: Rotational CARS spectra of $N_2$, $O_2$, and CO at room temperature, uncorrected for the broad-band laser spectrum. Some lines are assigned with the rotational quantum number of the lower level of the transition. Lower part: Computer simulations. All vertical scales are arbitrary

ing the spectrum of room temperature air. Lines corresponding to nitrogen and oxygen are marked (N) and (O), respectively. Except for a few coincidences all lines are well separated. The ratio of two line intensities in terms of the CARS amplitudes and the concentrations is

$$\frac{I_J(\mathrm{N})}{I_{\tilde{J}}(0)} = \left|\frac{c(\mathrm{N})}{c(\mathrm{O})} \cdot \frac{A_{J,J+2}(\mathrm{N})}{A_{\tilde{J},\tilde{J}+2}(\mathrm{O})}\right|^2 . \tag{13}$$

In this ratio all polarization dependent terms cancel and the ratio of the concentrations $c(\mathrm{N})/c(\mathrm{O})$ can be determined using the known polarizability anisotropies for $N_2$ (0.696 Å$^3$) and $O_2$ (1.099 Å$^3$) [25]. With the line pairs N4/O7, N8/O11, and N10/O15 from the spectrum in Fig. 3 the nitrogen content of air was calculated to be 79%, 76%, and 69%, respectively. This appears reasonable especially in view of the fact that the spectrum is uncorrected for the broad-band laser profile. In addition, the homogeneous line width of all transitions in both species was assumed equal. For practical applications one would exclude these sources of error through a calibration spectrum from a sample with known constitution.

The thermometric properties of rotational CARS were studied with $N_2$ since this is the thermometric substance employed in most vibrational CARS temperature measurements. $N_2$ was blown through an electric heater into an aluminum chamber with small holes for the entrance and exit of the laser beams. The temperature was measured with a thermometer in one corner of the sample chamber, which had been calibrated against a Pt-100 temperature dependent resistor placed at the position where the laser beams would cross. Spectra were taken in the range from room temperature to about 700 K. Our present equipment did not allow the simultaneous measurement of a reference spectrum. Therefore, spectra were averaged over several shots and the room-temperature spectrum taken as the reference: Comparison of the relative line intensities for all lines from $J=6$ to $J=20$ in the room-temperature spectrum with the calculated intensity pattern yielded correction factors which were subsequently used to normalize the spectra taken at higher temperatures. These corrected line intensities were fitted to the theoretical expression with the temperature as the adjustable parameter. This normalization procedure also corrects for any dependence of the line widths from the rotational quantum numbers.

Figure 4 shows rotational CARS spectra of $N_2$ at three different temperatures. To cover a broader spectral range, spectra obtained with two different settings of the center frequency of the monochromator were

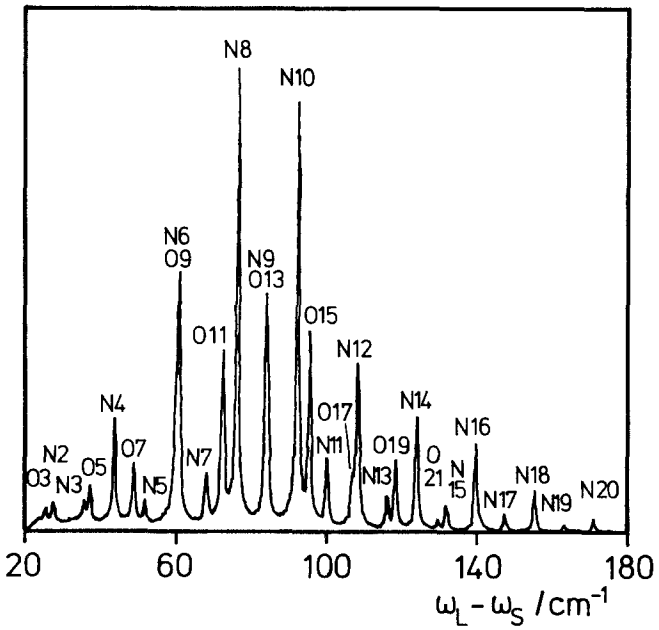


Fig. 3. Rotational CARS spectrum of air at room temperature. The lines are marked N and O for nitrogen and oxygen, respectively, followed by the rotational quantum number

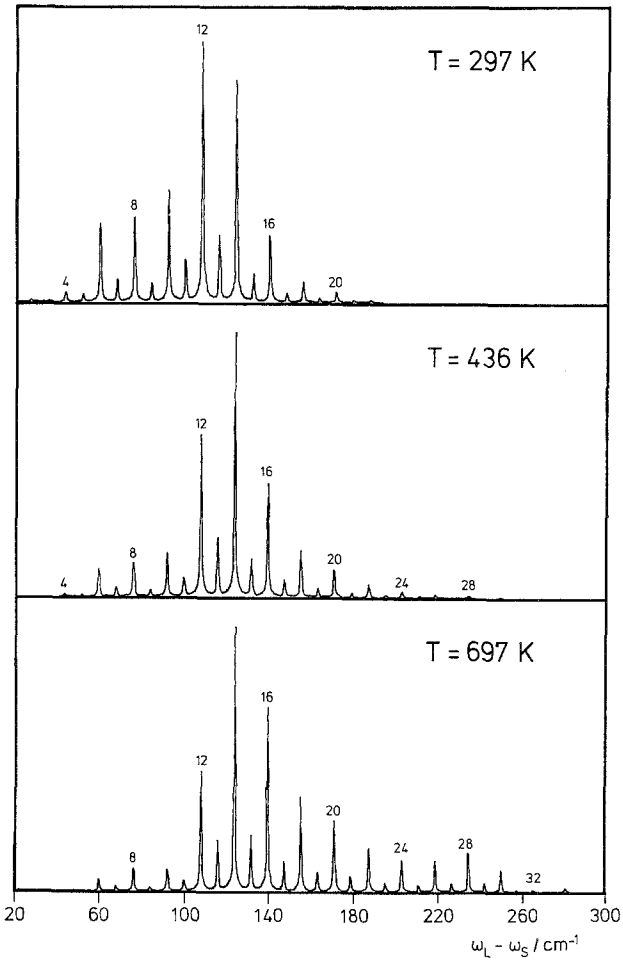


Fig. 4. Rotational CARS spectra of $N_2$ for three different temperatures. The center frequency of the broad-band dye laser was set to higher Stokes shifts, as compared to Figs. 2 and 3

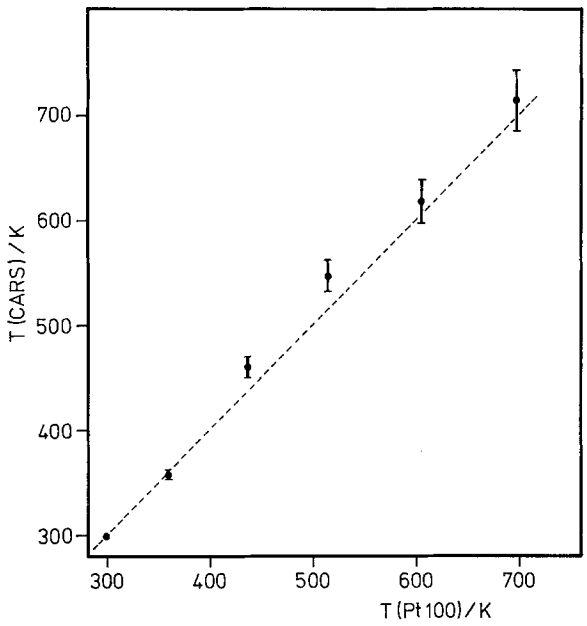


Fig. 5. Plot of the temperature determined from the rotational CARS spectra versus the temperature measured with a Pt-100 temperature dependent resistor

overlapped. The shift of spectral intensity to the higher transitions with increasing temperature is clearly visible. Figure 5 shows the plot of $T_{\mathrm{CARS}}$ vs. $T_{\mathrm{Pt\text{-}100}}$ obtained from the analysis of the spectra as described above. The error bars indicate one standard deviation from a fit based on 200 laser shots. This error increases monotonically with increasing temperature, i.e. with increasing distance from the reference. The dominant experimental contribution to this error is the shot-to-shot fluctuation in the spectrum of the broadband laser. This source of error could be largely eliminated with a simultaneous reference measurement. However, even in our present method the temperature fit appears to be reasonably good.

With increasing temperature the population differences for level pairs with $\Delta J=2$ will become rapidly smaller and rotational CARS signal intensities will drop to a low level despite the high rotational Raman cross section. In addition, a small change in temperature will have a lesser influence on the relative line intensities with increasing temperature. To estimate the importance of this effect we define a quantity $X$ as a measure of the change of the rotational CARS spectrum with a change in temperature

$$X(T, \Delta T)=\left\{\sum_J [I(J, T)-I(J, T+\Delta T)]^2\right\}^{1/2}. \qquad (14)$$

In this expression, $I(J, T)$ is the theoretical intensity of the rotational CARS line for the transition $J \rightarrow J+2$ at temperature $T$, normalized to the strongest line at this temperature. This quantity $X$ sets a limit to the allowed amount of noise and fluctuations in the experimental spectrum when a temperature fit with an accuracy of $\Delta T$ is required. Figure 6 shows curves of $X(T, \Delta T)$ as a function of temperature. Curve $a$ corresponds to a constant temperature accuracy $\Delta T$, curve $b$ to a constant relative temperature accuracy $\Delta T/T$. Both curves are normalized to 100 at $T=100$ K. The steep decay of curve $a$ indicates that the difference between two spectra with constant temperature difference $\Delta T$ decreases rapidly with increasing temperature. From 300 to 1000 K this decrease is by a factor of 5. Thus relative line intensities must be measured with 5 times the accuracy to yield the same accuracy in the temperature fit at 1000 K. The total signal intensity also drops by one order of magnitude in going to 1000 K, placing an even stronger restriction on the admissible signal-to-noise ratio. Curve $b$ shows that the situation is somewhat better when constant relative temperature accuracy $\Delta T/T$ is required. With a constant accuracy

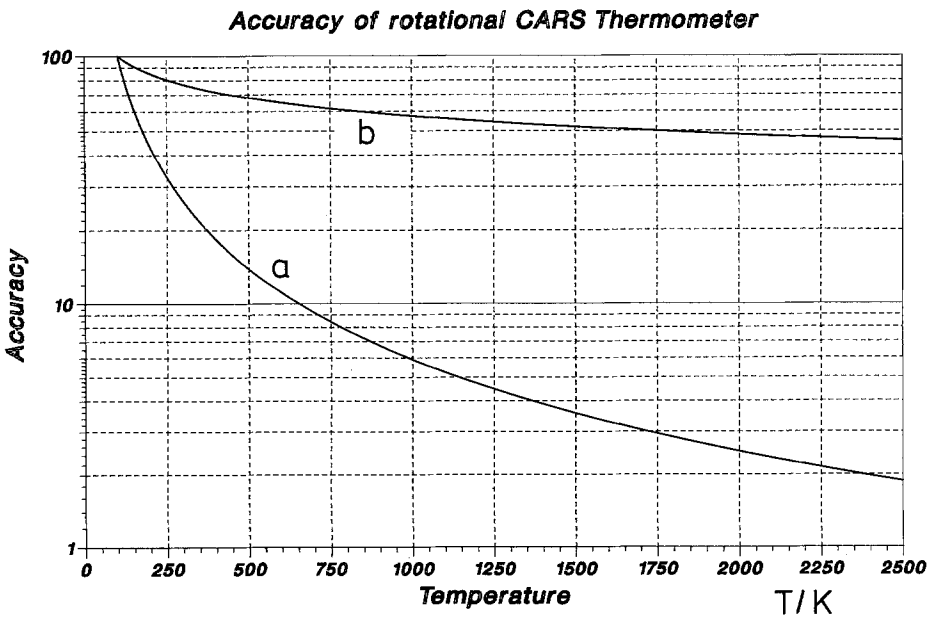


Fig. 6. Plot of the quantity $X(T, \Delta T)$ as the admittable error in relative line strength measurements for a given accuracy of the temperature fit for rational CARS spectra

in the relative line-strength measurement the uncertainty in the temperature fit will increase with temperature, in complete agreement with our findings in Fig. 5.

## 4. Conclusions

Pure rotational CARS has been shown to yield a snapshot of the population distribution in individual rotational levels of diatomic molecules. Thermometry up to 700 K has been demonstrated with possible extension to much higher temperatures. (We have obtained rotational CARS spectra of $N_2$ in flames of $CH_4$ in air, but we found vibrational CARS to be definitely superior for thermometry in this higher temperature range.) Another possible application of rotational CARS is the analysis of the product state distribution in molecular beam collision experiments, or gas phase photochemistry with $N_2$ as leaving group. Molecules with similar rotational constants like $N_2$, $O_2$, and CO have overlapping spectra. Therefore, in mixtures with many components rotational CARS spectra will be difficult to interprete. On the other hand, this allows species identification and concentration measurements in mixtures with few components.

The choice of the excimer laser pumped dye laser system is not essential to this kind of spectroscopy. Probably, a Nd:YAG laser system would have been even easier to operate. However, in such a system the pump beam frequency is fixed to the Nd:YAG laser second harmonic frequency, whereas the excimer laser based system allows independent tuning of both beams interacting in the CARS process. This can be an advantage when electronic resonance enhancement can be achieved through the appropriate choice of the pump beam frequency. In this way CARS spectra of particular low concentration intermediates in reactive media can be selectively obtained [26, 27].

*Acknowledgements.* We are indebted to Lambda Physik (Göttingen) and Mitsubishi Heavy Industries (Nagasaki) for giving us the opportunity to work with their prototype CARS apparatus. The loan of the double monochromator (Spex, Munich) and a methane burner (Prof. Wolfrum, Heidelberg) is also greatly acknowledged. Many thanks are to Prof. Marowsky for negotiating these loans and providing other equipment, especially the nitrogen heater chamber.

## References

1. D.R. Crosley (ed.): *Laser Probes for Combustion Chemistry.* ACS Symposium Series (American Chemical Society, Washington, DC 1980)
2. A.C. Eckbreth, P.A. Bonczyk, J.F. Verdieck: Prog. Energ. Combust. Sci. **5**, 253 (1979)
3. A.C. Eckbreth: Combust. Flame **39**, 133 (1980)
4. S. Druet, J.-P. Taran: Prog. Quantum Electron. **7**, 1 (1981)
5. R.J. Hall, A.C. Eckbreth: Opt. Eng. **20**, 494 (1981)
6. T.R. Gilson, I.R. Beattie, J.D. Black, D.A. Greenhalgh, S.N. Jenny: J. Raman Spectrosc. **9**, 361 (1980)
7. R.L. Farrow, P.L. Mattern, L.A. Rahn: Appl. Opt. **21**, 3119 (1982)
8. A.C. Eckbreth, R.J. Hall: Combust. Flame **36**, 87 (1979)
9. R.J. Hall, L.R. Boedeker: Appl. Opt. **23**, 1340 (1984)
10. M. Pealat, P. Bouchardy, M. Lefebvre, J.-P. Taran: Appl. Opt. **24**, 1012 (1985)
11. J.J. Barrett: Appl. Phys. Lett. **29**, 722 (1976)
12. K. Aron, L.E. Harris, J. Fendell: Appl. Opt. **22**, 3604 (1983)
13. I.R. Beattie, T.R. Gilson, D.A. Greenhalgh: Nature **276**, 378 (1978)
14. C.M. Roland, W.A. Steele: J. Chem. Phys. **73**, 5919 (1980)
15. L.P. Goss, J.W. Fleming, A.B. Harvey: Opt. Lett. **5**, 345 (1980)
16. J.A. Shirley, R.J. Hall, A.C. Eckbreth: Opt. Lett. **5**, 380 (1980)
17. M. Alden, H. Edner, S. Svanberg: Phys. Scr. **27**, 29 (1983)
18. J.B. Zheng, A. Leipertz, J.B. Snow, R.K. Chang: Opt. Lett. **8**, 350 (1983)
19. J.B. Snow, J.B. Zheng, R.K. Chang: Opt. Lett. **8**, 599 (1983)
20. D.V. Murphy, R.K. Chang: Opt. Lett. **6**, 283 (1981)
21. J.B. Zheng, J.B. Snow, D.V. Murphy, A. Leipertz, R.K. Chang, R.L. Farrow: Opt. Lett. **9**, 341 (1984)
22. M.A. Yuratich: Mol. Phys. **38**, 625 (1979)
23. Y. Prior: Appl. Opt. **19**, 1741 (1980)
24. G. Herzberg: *Molecular Spectra and Molecular Structure, I: Spectra of Diatomic Molecules* (Van Nostrand, New York 1950)
25. N.J. Bridge, A.D. Buckingham: Proc. R. Soc. London A **295**, 334 (1966)
26. S. Druet, B. Attal, T.K. Gustafson, J.-P. Taran: Phys. Rev. A **18**, 1529 (1978)
27. B. Attal, D. Debarre, K. Mueller-Dethlefs, J.-P.E. Taran: Rev. Phys. Appl. **18**, 39 (1983)